

# Seismic Performance of Precast Concrete Special Moment Frames with Hybrid Connection System in Five and Ten Story Buildings

Chandra, J.<sup>1\*</sup>, Lokito, V.N.<sup>1</sup>, and Tambuna, J.A.<sup>1</sup>

**Abstract:** Precast concrete has been widely implemented in various construction projects due to shorter construction duration and consistent quality. In a previous study, Solberg et al. (2008) conducted an experiment on hybrid beam-column connections with *Damage Avoidance Design* concept to improve the seismic performance of precast concrete special moment frames. The objective of this study is to further evaluate the seismic performance of precast concrete special moment frames with the hybrid beam-column connections in five and ten story buildings. The evaluation was done through non-linear dynamic time history analysis using OpenSees. The analysis results show that precast concrete frame buildings exhibit insignificant difference in maximum interstory drift ratios and roof displacements as compared to conventional concrete frame buildings. However, with significantly smaller residual displacements which indicates less structural damage, precast concrete frame buildings could be preferred in the long run as they require less structural repairs after a strong earthquake event.

**Keywords:** Precast concrete special moment frame; hybrid beam-column connections; *Damage Avoidance Design*; seismic performance.

## Introduction

Precast concrete structures have started to be implemented on a multitude of construction projects across the globe. Such a phenomenon was due to the relatively shorter construction period, consistently higher grade of elements, and the lower need of formwork, which translates into a relatively more efficient construction [1].

The seismic performance of precast concrete structures however depends strongly on their connections, especially on their beam-column connections. Therefore, to maintain both lateral force capacity and repairability, multiple researches have been done by Precast Seismic Structural Systems (PRESSS), which have shown sufficient performance by hybrid connections [2]. Gap opening and self-centering properties of hybrid connections allow structures to temporarily sway in a controlled fashion to dissipate energy and reduce residual deformation. The *Damage Avoidance Design* concept then was brought by Mander and Cheng [3], which reinforced element surfaces to mitigate element damages such as concrete crushing.

Such concept was developed further by Solberg et al. [4], which proposed a precast concrete beam-column hybrid connection with unbonded post-tensioning tendons and external dissipation devices. The conducted experiment showed high performance capabilities of the hybrid precast connection with minor non-structural damage to the precast concrete beam at 2% drift, and controlled damages, such as steel dissipator yielding, concrete spalling, and post-tensioning loss, at 4.7% drift.

However, despite its research outcome, few research has been conducted to simulate the performance of such hybrid connection in a complete precast concrete structure. This research is then conducted to assess, in a macro-modelling approach, the performance of the hybrid precast connection proposed by Solberg et al. [4] in typical five and ten story precast concrete buildings.

## Damage Avoidance Design of Beam-Column Connection

The east-west direction specimen detail of the hybrid beam-column connection with *Damage Avoidance Design* proposed by Solberg et al. [4] is displayed in Figure 1. The specimen consists of a column and two precast seismic beams in the east-west direction and one gravity beam in the north-south direction. In this study, only the seismic beams were taken into consideration.

The mentioned specimen was a 80% constant stress and strain similitude scaled second floor exterior joint

<sup>1</sup> Civil Engineering Department, Faculty of Civil Engineering and Planning, Petra Christian University, Jl. Siwalankerto 121-131, Surabaya 60236, INDONESIA.

\*Corresponding author; Email: [chandra.jimmy@petra.ac.id](mailto:chandra.jimmy@petra.ac.id)

**Note:** Discussion is expected before November, 1<sup>st</sup> 2023, and will be published in the "Civil Engineering Dimension", volume 26, number 1, March 2024.

Received 10 May 2023; revised 10 June 2023; accepted 09 August 2023.

of a ten story building. The 700 x 700 mm<sup>2</sup> column was given four 32 mm post-tensioned high strength threaded bars to simulate axial load of 2000 kN with longitudinal reinforcement of 12D20. The 400 x 560 mm<sup>2</sup> precast beams had two 26.5 mm high strength threaded bars located inside 50 mm PVC duct at a third of the beam height. Additional 15 mm diameter mild steel energy dissipation devices were installed on the sides. Straight couplers were utilized to connect bolt bars at the beam-column connection with a bent post-tensioning tendon with a 1.8 m radius. A 75% mechanically reduced high strength threaded bar was utilized as a bolt bar, which was installed through a duct for easy replacement. As a *Damage Avoidance Design* connection system, L 100x100x12 plates were installed at the top and bottom of each beam face to prevent beam element damage. At each connection, four shear keys with 30 mm diameter were installed with a slight angle of 5 degrees to prevent impact when rocking.

The moment capacity of the hybrid beam-column connection may be expressed as the resultant of the contribution of the unbonded post-tensioned tendons and the external dissipation devices as shown in Equation 1. Each moment contribution of the unbonded post-tensioned tendons and external dissipation devices are considered as the product of both the prestress and dissipator force and their eccentricity towards the connection's rotation edge, as stated in Equations 2 and 3 [1].

$$M_{con}^{\pm} = M_{ps}^{\pm} + M_{diss}^{\pm} \quad (1)$$

$$M_{ps}^{\pm} = P_{ps}^{\pm} \times e_{ps}^{\pm} \quad (2)$$

$$M_{diss}^{\pm} = P_{diss}^{\pm} \times e_{diss}^{\pm} \quad (3)$$

Where  $M_{ps}^{\pm}$  and  $M_{diss}^{\pm}$  are the moment capacity of the post-tensioned tendons and the external dissipation devices.  $P_{ps}^{\pm}$  and  $P_{diss}^{\pm}$  are prestressed force and dissipator force, respectively.  $e_{ps}^{\pm}$  and  $e_{diss}^{\pm}$  are the eccentricity of each component about the rocking edges.

The prestressed force of the unbonded post-tensioned tendons is determined from the size of the gap-opening and initial prestressed force of the tendons, as in Equation 4. As the gap opens, the post-tensioning tendon force increases until it reaches its yielding point. The connection rotation correlated to the tendon's yielding point could be defined in Equation 5. To achieve sufficient maximum energy dissipation capacities while maintaining the connection's self-centering properties, the moment capacity of the post-tensioned tendons must exceed the moment capacity of the steel dissipation devices by a factor of  $\lambda_{diss}$ , as written in Equation 6 [1].

$$P_{ps}^{\pm} = P_{ps\_initial} + \frac{A_{ps}E_{ps}}{L_t} e_{ps}^{\pm} |\theta_{con}| \quad (4)$$

Where  $P_{ps\_initial}$  is the initial prestressing force;  $A_{ps}$  is the total area of the prestressed tendon;  $E_{ps}$  is the elastic modulus of the tendon;  $L_t$  is the length of the unbonded tendon;  $\theta_{con}$  is the connection rotation.

$$|\theta_{con\ yield}^{\pm}| = \frac{f_y - \frac{P_i}{A_{boltbar}}}{E_{ps} \times e_{ps}^{\pm} \times 2} \left( \frac{A_{boltbar}}{A_{ps}} \right) L_t \quad (5)$$

In which  $f_y$  is the tendon yielding stress;  $P_i$  is the initial tendon force;  $A_{boltbar}$  is the area of bolt bar.

$$\lambda_{diss} M_{diss}^{\pm} < f M_{ps}^{\pm} \quad (6)$$

To complement the self-centering properties of the beam-column joints, the column-foundation connection must be able to resist and transfer gravity and seismic forces from the column with sufficient energy dissipation and self-centering capabilities. Therefore, as addition, the column-foundation joint was designed following a hybrid shoe block at pier with *Damage Avoidance Design* proposed by Solberg [5]. The specimen was a 30% scaled 7 meters bridge pier. The connection consists of a head block, shoe block, and base block. The base block-shoe block connection was armoured with a 32 mm thick 700x700 mm<sup>2</sup> steel plate. The connection was also complemented with unbonded post-tensioning tendons and energy dissipation devices. The shoe block connection could be seen in Figure 2.

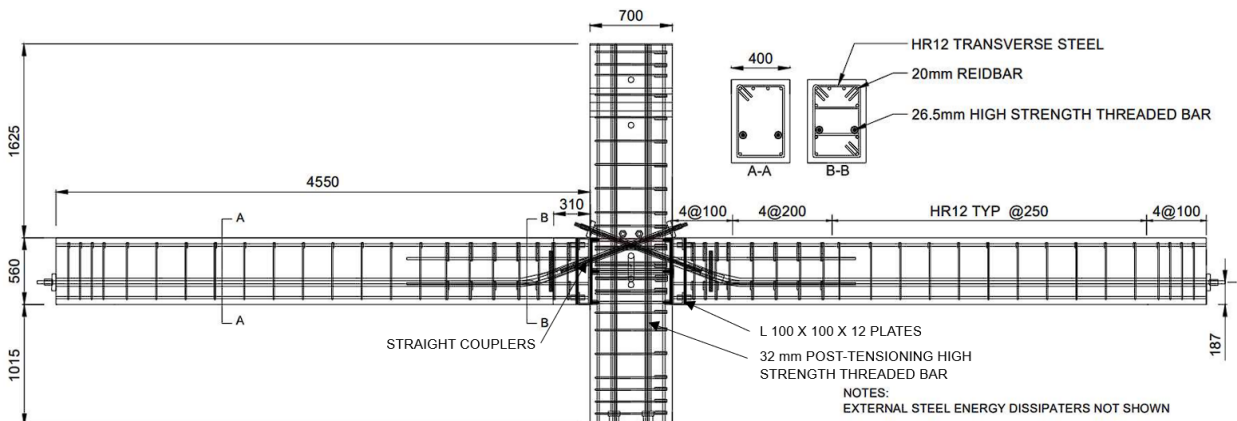


Figure 1. Specimen Detail in the East-west Direction of the Hybrid Beam-column Joint with *Damage Avoidance Design* [4]

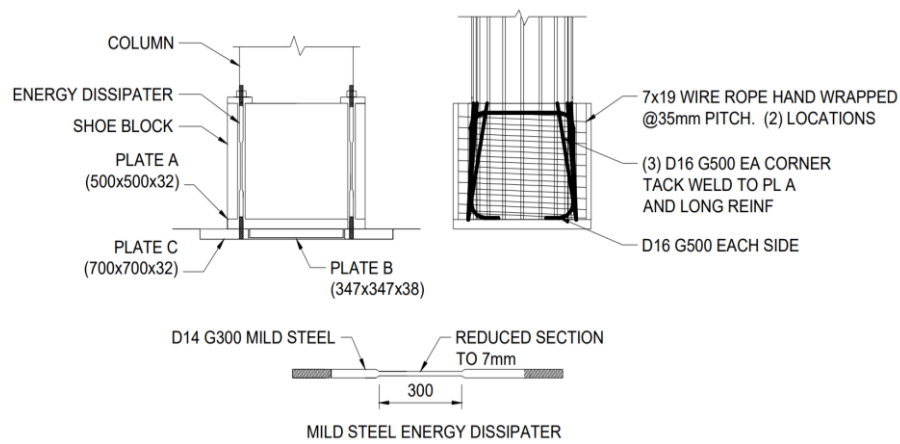


Figure 2. Specimen Detail of the Hybrid Column-foundation Joint with *Damage Avoidance Design* [5]

### Considered Buildings

In this study, two 5 and 10 story typical office buildings were designed as monolithic concrete structures and precast concrete structures. While the precast concrete structures were used to analyse the performance of the hybrid beam-column connection proposed by Solberg et al. [4], the monolithic concrete structures were also analysed as comparison. Monolithic concrete structures are coded as CIP5 and CIP10, and the precast concrete structures are coded as PC5 and PC10. The numbers behind the notations represent the number of story in each building. Each building has four 8 meter bays in the X direction and six 6 meter bays in the Y direction, with a constant floor elevation of 3.5 meters. Floor plan of the evaluated buildings can be seen in Figure 3.

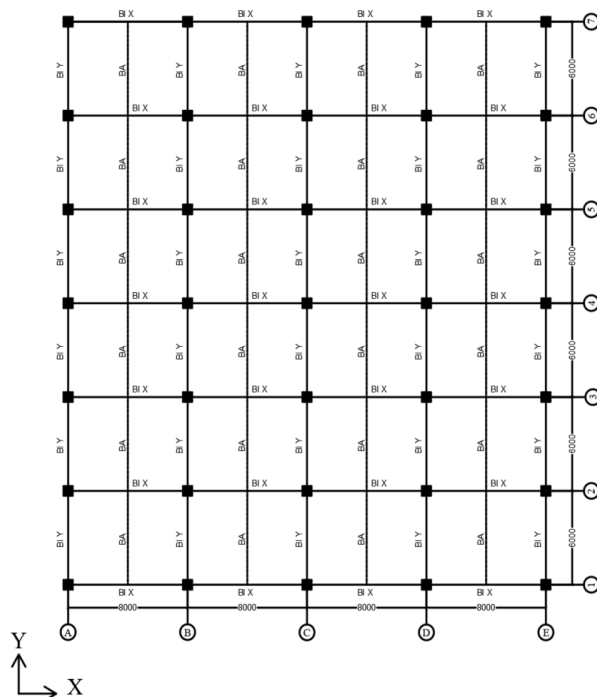


Figure 3. Building Floor Plan

The live load applied was based on SNI 1727:2020 [6], and the dead loads considered the structure’s self-weight and finishing loads. The dimensions of the beams used were 400 x 750 mm<sup>2</sup> for the X frame beams and 400 x 600 mm<sup>2</sup> for the Y frame beams. For the 5 story buildings 600 x 600 mm<sup>2</sup> columns were used for each story, while the 10 story buildings used 700 x 700 mm<sup>2</sup> columns for the lower 6 stories and 600 x 600 mm<sup>2</sup> columns for the rest. All buildings were designed with concrete strength,  $f_c$ , of 35 MPa and steel bar strength,  $f_y$ , of 420 MPa. High strength threaded bars from MacAlloy™ were used as the unbonded post-tensioning tendons in this study.

Structural models for both cast in place and precast concrete buildings are quite similar since in the precast concrete buildings, due to the nature of post-tensioning and the presence of clamping forces, the connections between beams and columns could be assumed as rigid connections as in the case of cast in place concrete buildings. Post-tensioning effects occur majorly only on the non-linear phase of the connections, which is indicated by gap openings [1]. The monolithic cast in place buildings were designed as special concrete moment frames according to ACI 318-14 [7], which is the equivalent of SNI 2847:2019 [8]. The precast concrete buildings however were designed according to the design procedures proposed by Solberg et al. [4]. Each beam-column connection of the precast buildings was designed according to the hybrid beam-column connection with *Damage Avoidance Design* proposed by Solberg et al. [4]. It is worth noting that the precast concrete beams were designed to have same positive and negative moment capacities at their ends due to their rocking motion. This was done to allow equal beam rotations at both directions.

To complement the self-centering properties of the beam-column connections, the column-foundation joints were also designed according to hybrid shoe

block at pier *Damage Avoidance Design* connections. In addition, the precast concrete buildings were also designed implementing Strong Column-Strong Beam-Weak Connection philosophy. Detailed information on the designed hybrid beam-column and shoe block connections used in this study is shown in Table 1. The corresponding reinforcement result and beams' demand to capacity ratio of both buildings are shown in Tables 2 and 3, respectively.

For this study, the ground motion record used was taken from the Imperial Valley 1940 earthquake recorded in El-Centro USGS station 117. The ground motion was scaled to the  $MCE_R$  response spectrum located in Surabaya with soil class E using Spectral Matching method, as displayed in Figure 4.

### Modelling Approach

The evaluated buildings were modelled using OpenSees software (Open System for Earthquake Engineering Simulation) due to its multitude of materials, elements, modelling methods, and efficiency in analysis. The material "Self-Centering Material-Flag-Shaped Hysteresis" introduced by Jeff Erochko to support the research by Christopoulos et al. [9] was

chosen to represent the self-centering characteristics of the hybrid beam-column connection with *Damage Avoidance Design*.

In cast in place concrete buildings, beams and columns were modelled using "Beam with Hinges" elements [10]. "Beam with Hinges" was chosen due to its capability to divide any element into 3 parts: 2 plastic hinge regions at both ends and an elastic region at the center, with the flexibility to determine the assumed plastic hinge length [11]. While the elastic region was represented with "Elastic Section" with "Elastic Uniaxial Material", "Section Aggregator" containing Fiber Section and Elastic Uniaxial Material was used to model the plastic hinge regions. Materials "Concrete02" and "Steel02" were used to model the fiber sections.

In precast concrete buildings, beams and columns were also modelled using "Beam with Hinges" elements. The beam ends were modelled for the self-centering characteristics of the hybrid connection, using the material "Self-Centering Material-Flag-Shaped Hysteresis" to represent the major axis moment capacity, combined with 5 other "Elastic Uniaxial Material", to represent the other properties

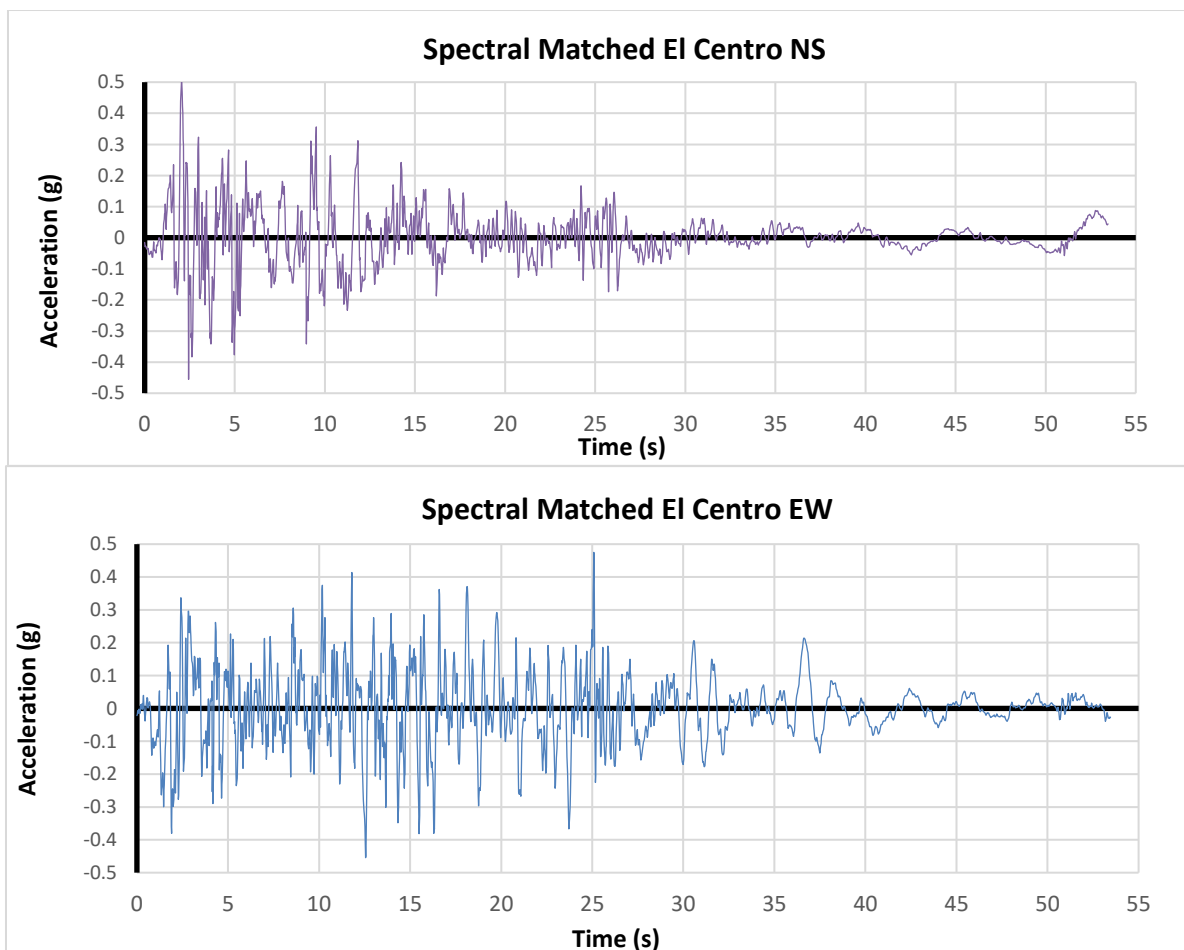


Figure 4. Spectral Matched El-Centro 1940 Earthquake Acceleration Records

(minor axis bending, shear, axial, and torsion), in a section aggregator with an assumed length equivalent to the beam height. On the other hand, the columns were modelled similarly to cast in place buildings, using “Beam with Hinges” elements with fiber sections for each column ends and elastic uniaxial sections for the column’s elastic region. In addition, the column-foundation connection was modelled using “Self-Centering Material-Flag-Shaped Hysteresis” to mimic the shoe block connection.

### Modelling Verification

To verify that the proposed modelling method was sufficient to represent the behavior of the hybrid beam-column connection, the hysteresis curve achieved from the original experiment [4] was compared with the generated hysteresis curve from the analysis using OpenSees. The validation process was done on the quasi-static bidirectional “clover leaf” test results on the seismic EW beam. Figure 5 displays the comparison of hysteresis curves generated from OpenSees against the experiment results. Although the stiffness of the modelled connection was deemed accurate due to the similar gradient of linear and non-linear phase with the experiment results, it should be noted that the transition of both phases was depicted as an intercept between two straight lines, rather than a gradual parabolic curve. The proposed modelling did not show any signs of residual displacement of 0.1% as seen in the experiment results. However, such inaccuracy was deemed acceptable since the recorded residual displacement of 0.1% in the experiment was due to the unexpected 2 mm drift of the column base pin.

### Seismic Performance Evaluation Results

In total, four buildings were investigated against two schemes of non-linear time history analysis (NLTHA). To represent accurate earthquake simulations, the spectral matched ground motions were applied in both orthogonal directions of the buildings as stated in ASCE 41-17 [12]. Due to the asymmetrical plan of the buildings, two schemes of analysis were conducted for each building. For the first scheme, the North-South ground motion was applied at the X axis of the building, while the East West ground motion was applied at the Y axis of the building. The second scheme switches the applied axis of the ground motion pair. Based on the severity of the results, the second scheme was chosen to be displayed in this paper.

The maximum interstory drift ratio and residual displacement of the five and ten story buildings are shown in Figures 6 and 7. It could be seen that all evaluated buildings meet the maximum  $MCE_R$  drift limitation of 4% according to ASCE 7-16 [13]. In terms of its maximum interstory drift ratio, precast concrete (PC) buildings perform similarly to cast in place concrete (CIP) buildings, without any significant difference. The maximum roof displacements of PC buildings were found to be slightly higher than CIP buildings, which indicate a more flexible nature of precast concrete structures. This is due to the lower nonlinear phase stiffness value of the hybrid connections compared to monolithic cast in place beam-column connections. The residual roof displacements however highlight the superiority of PC buildings. In all evaluated buildings, PC buildings were recorded to

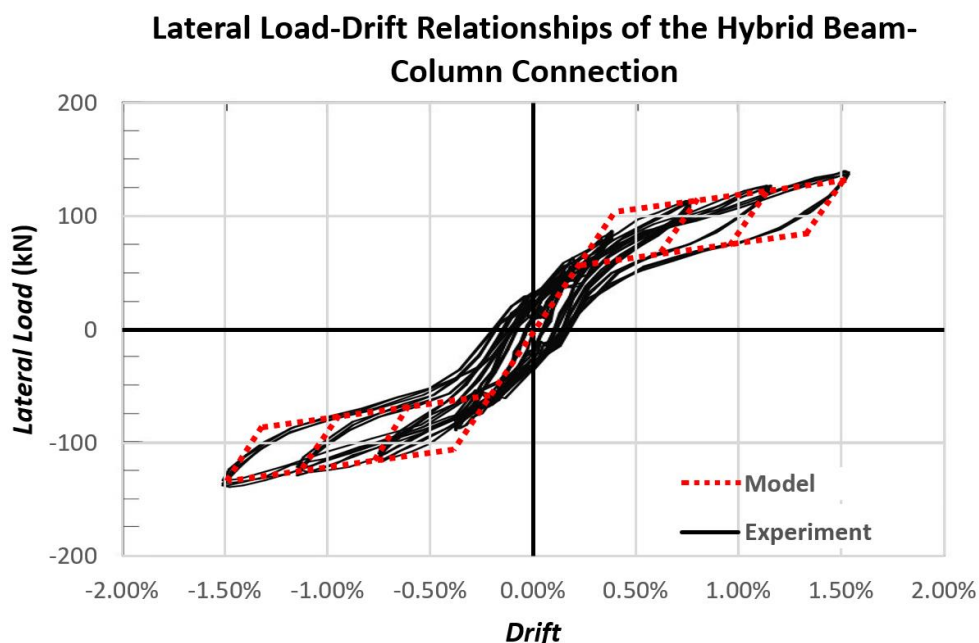


**Figure 5.** Verification of the Proposed Modelling for the Hybrid Beam-column Connection

have substantially lower residual roof displacements, which on average are 97.4% less than its CIP counterparts. This indicates that PC buildings suffer significantly less damage as compared to CIP buildings.

Table 4 displays the maximum roof displacements during the evaluation. It could be seen that precast concrete buildings were recorded to have relatively higher maximum roof displacements compared to

**Table 1.** Hybrid Beam-column Connection and Shoe Block Connection Design for 5 and 10 Story Precast Buildings

Story	Type	Dimension	5 story precast building				10 story precast building			
			Tendon	Bolt Bar	fpse	Energy Dissipation Devices	Tendon	Bolt Bar	fpse	Energy Dissipation Devices
1	BIX	400 x 750	D36	D33.5	42%fy	D28	D36	D34	41%fy	D28
2	BIX	400 x 750	D36	D33.5	42%fy	D28	D40	D37.5	35%fy	D28.5
3	BIX	400 x 750	D32	D30.5	47%fy	D27	D40	D37.5	35%fy	D28.5
4	BIX	400 x 750	D32	D29	47%fy	D25	D40	D37.5	35%fy	D28.5
5	BIX	400 x 750	D26.5	D25.5	51%fy	D23	D40	D37	35%fy	D27.5
6	BIX	400 x 750					D40	D36	36%fy	D27
7	BIX	400 x 750					D36	D33.5	39%fy	D27
8	BIX	400 x 750					D32	D30.5	42%fy	D25.5
9	BIX	400 x 750					D32	D30	43%fy	D25
10	BIX	400 x 750					D26.5	D26	47%fy	D23
1	BIY	400 x 600	D32	D29.5	40%fy	D24	D32	D30	40%fy	D25
2	BIY	400 x 600	D32	D29.5	40%fy	D24	D36	D33.5	34%fy	D25
3	BIY	400 x 600	D32	D27.5	44%fy	D23	D36	D33.5	34%fy	D25.5
4	BIY	400 x 600	D26.5	D24	46%fy	D21	D36	D33.5	34%fy	D25.5
5	BIY	400 x 600	D22	D21	46%fy	D18	D36	D33.5	36%fy	D25.5
6	BIY	400 x 600					D36	D32.5	41%fy	D24.5
7	BIY	400 x 600					D32	D30	45%fy	D24
8	BIY	400 x 600					D32	D28	44%fy	D22.5
9	BIY	400 x 600					D26.5	D25	46%fy	D22
10	BIY	400 x 600					D26.5	D24	45%fy	D21
1	Corner Shoe block	700 x 700	D40	-	40%fy	D10	D40	-	0%fy	-
1	Exterior Shoe block	700 x 700	D40	-	40%fy	D10	D40	-	0%fy	-
1	Interior Shoe block	700 x 700	D20	-	29%fy	D10	D20	-	0%fy	-

**Table 2.** End Section Longitudinal Reinforcement Results of 5 and 10 Story Buildings

Story	Element	Dimensions	Cast in Place Building (CIP5)		Precast Building (PC5)		Cast in Place Building (CIP10)		Precast Building (PC10)	
			Top	Bottom	Top	Bottom	Top	Bottom	Top	Bottom
1		400 x 750	7D22	4D22	7D22	7D22	7D22	3D22	7D22	7D22
2		400 x 750	7D22	4D22	7D22	7D22	7D22	4D22	8D22	8D22
3		400 x 750	6D22	3D22	6D22	6D22	8D22	4D22	8D22	8D22
4		400 x 750	6D22	3D22	5D22	5D22	8D22	4D22	8D22	8D22
5		400 x 750	5D22	3D22	4D22	4D22	7D22	4D22	8D22	8D22
6	BIX	400 x 750					7D22	4D22	7D22	7D22
7		400 x 750					7D22	3D22	7D22	7D22
8		400 x 750					6D22	3D22	6D22	6D22
9		400 x 750					5D22	3D22	5D22	5D22
10		400 x 750					4D22	3D22	4D22	4D22
1		400 x 600	5D22	3D22	6D22	6D22	5D22	3D22	5D22	5D22
2		400 x 600	5D22	3D22	6D22	6D22	6D22	4D22	7D22	7D22
3		400 x 600	5D22	3D22	5D22	5D22	6D22	4D22	7D22	7D22
4		400 x 600	4D22	2D22	4D22	4D22	6D22	4D22	7D22	7D22
5		400 x 600	3D22	2D22	3D22	3D22	6D22	4D22	7D22	7D22
6	BIY	400 x 600					6D22	3D22	6D22	6D22
7		400 x 600					5D22	3D22	5D22	5D22
8		400 x 600					4D22	2D22	4D22	4D22
9		400 x 600					4D22	2D22	4D22	4D22
10		400 x 600					3D22	2D22	3D22	3D22
1		700 x 700		24D22		20D22		24D22		28D25
2		700 x 700		16D22		20D22		16D22		28D25
3		700 x 700		16D22		20D22		16D22		24D22
4	COL I	700 x 700		16D22		16D22		16D22		20D22
5		700 x 700		16D22		12D22		16D22		20D22
6		700 x 700						16D22		20D22
7		600 x 600						16D22		24D22
8		600 x 600						16D22		20D22
9	COL II	600 x 600						12D22		20D22
10		600 x 600						12D22		12D22

**Table 3.** Beams’ Demand to Capacity Ratios of 5 and 10 Story Buildings

Story	Element	Dimensions	Cast in Place Building (CIP5)	Precast Building (PC5)	Cast in Place Building (CIP10)	Precast Building (PC10)
1	BIX	400 x 750	0.65	0.96	0.75	0.92
2		400 x 750	0.66	0.93	0.85	0.89
3		400 x 750	0.73	0.96	0.77	0.90
4		400 x 750	0.69	0.93	0.77	0.89
5		400 x 750	0.74	0.92	0.87	0.91
6		400 x 750			0.84	0.90
7		400 x 750			0.81	0.91
8		400 x 750			0.89	0.95
9		400 x 750			0.99	0.88
10		400 x 750			0.86	0.87
1	BIY	400 x 600	0.71	0.93	0.56	0.89
2		400 x 600	0.81	0.93	0.61	0.90
3		400 x 600	0.82	0.96	0.71	0.91
4		400 x 600	0.92	0.92	0.69	0.89
5		400 x 600	0.85	0.85	0.65	0.88
6		400 x 600			0.71	0.86
7		400 x 600			0.74	0.87
8		400 x 600			0.76	0.87
9		400 x 600			0.75	0.86
10		400 x 600			0.73	0.84

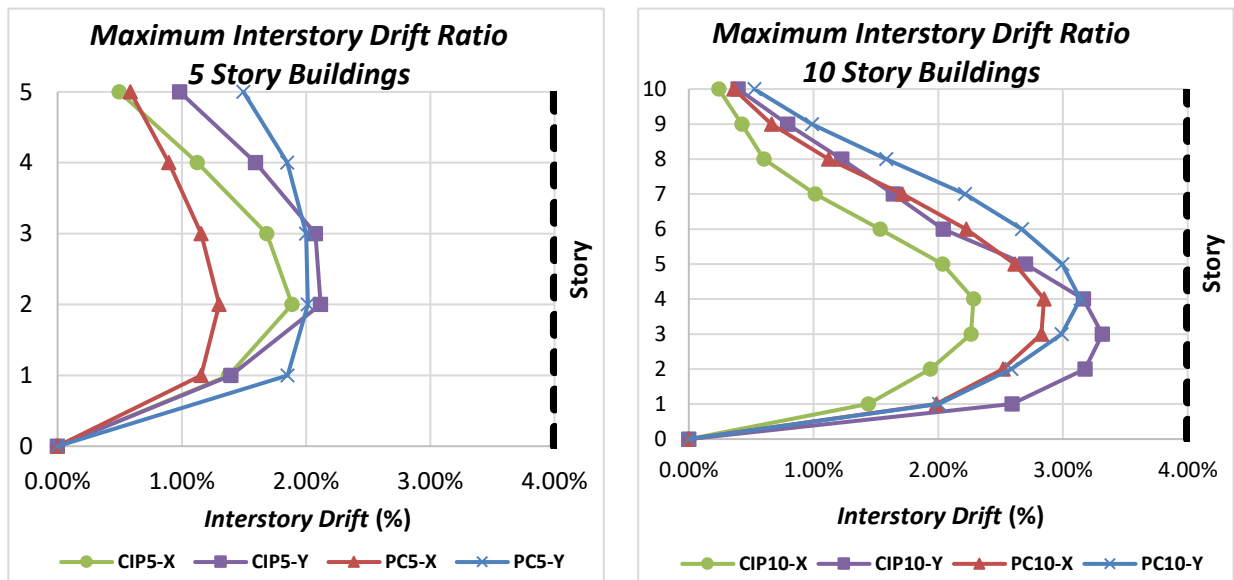


**Figure 6.** Maximum Interstory Drift Ratio of All Evaluated Buildings

cast in place concrete buildings, except for 5 story building in the X direction. While the maximum roof displacement differences for the Y frame were recorded to be just below 4 percent, a much larger difference is visible for the X frame. Since the demand to capacity ratios, building periods, and base shears were not significantly different for the two frames, this might happen due to the asymmetrical building layout and the chosen second earthquake loading scheme.

According to ASCE 41-17 [12], the plastic hinge formations of the evaluated buildings were found to be satisfactory, with no connection exceeding collapse prevention. Some interior and exterior frame examples can be seen in Tables 5 and 6 for 5 and 10 story buildings, respectively. As previously shown in the maximum displacements and maximum interstory

drift ratios, the X direction frames tend to perform better compared to the Y direction frames. This is confirmed through less plastic hinge damages in the X direction frames.

Compared to CIP frames, PC frames tend to have evenly distributed higher hinge rotations across their connections. This was due to the “rocking” nature of the hybrid connections. Since plastic hinge conditions are based on the maximum observed plastic hinge rotations, the classification might overlook the self-centering capabilities of the hybrid connections, which could potentially underestimate the performance of the hybrid connections. Therefore, in this study, the evaluation of plastic hinge conditions for PC frames is based on the rotation limits at which the connection gap starts to open and when the bolt bar starts to yield.

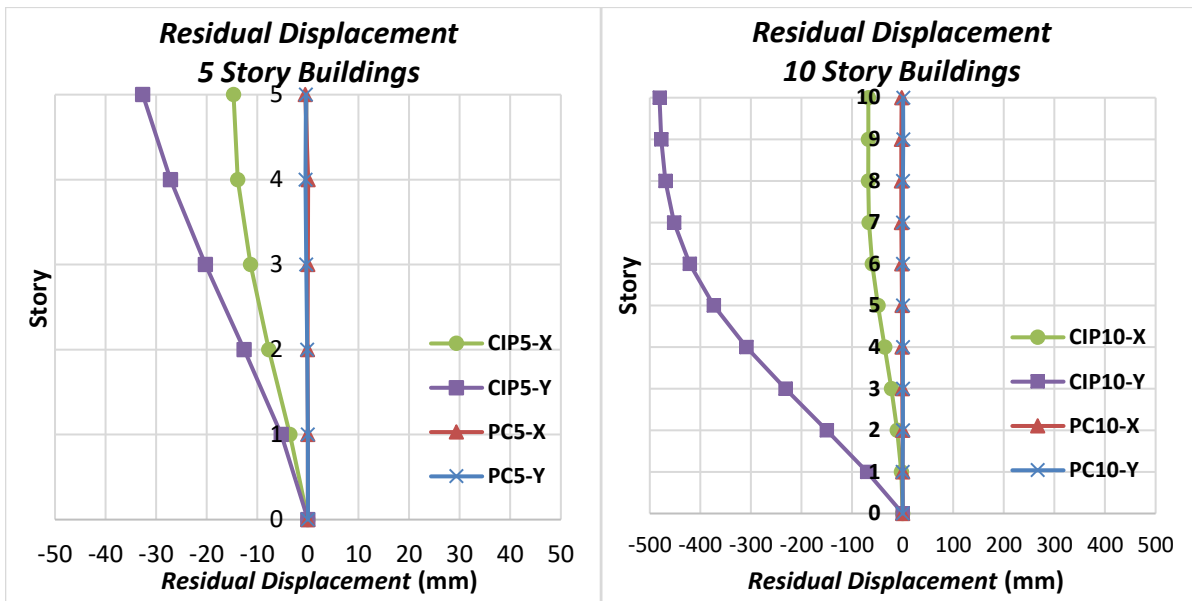
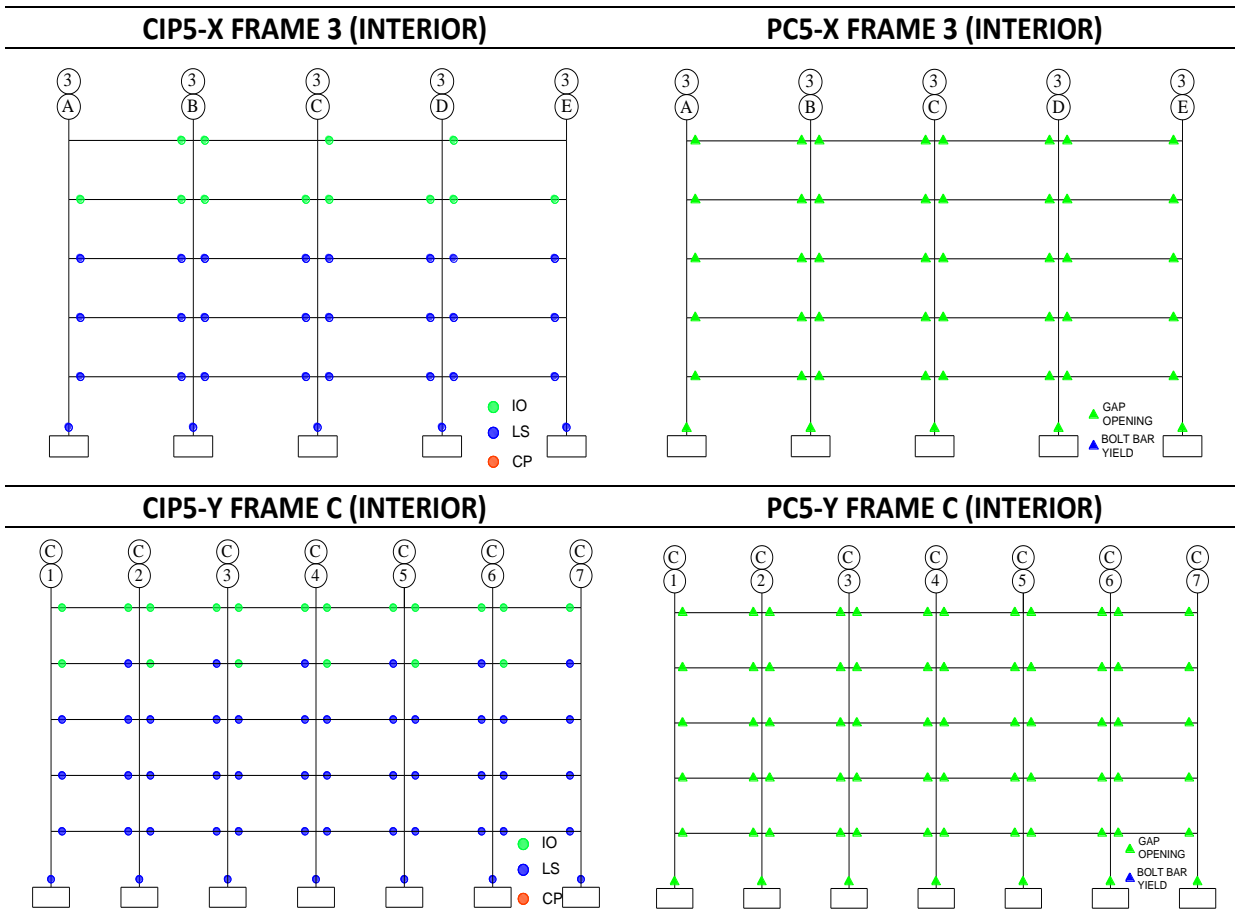


Figure 7. Residual Displacement of All Evaluated Buildings

Table 4. Maximum Roof Displacement of All Evaluated Buildings.

	CIP-X (mm)	CIP-Y (mm)	PC-X (mm)	PC-Y (mm)	X Frame Difference	Y Frame Difference
5 Story	227.4	280.8	167.7	291.8	-26.3%	3.9%
10 Story	461.0	702.1	653.6	728.3	41.8%	3.7%

Table 5. Plastic Hinge Formation of 5 Story Buildings



**Table 6.** Plastic Hinge Formation of 10 Story Buildings

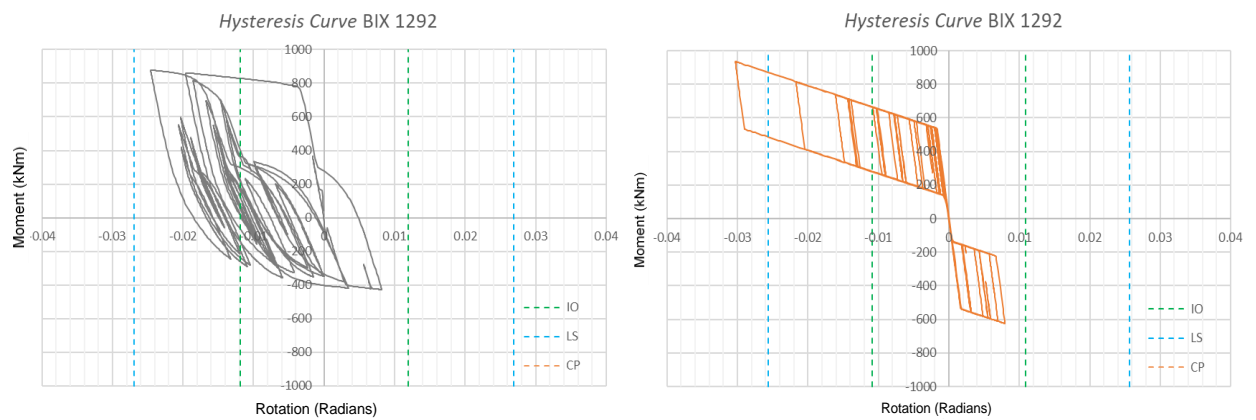
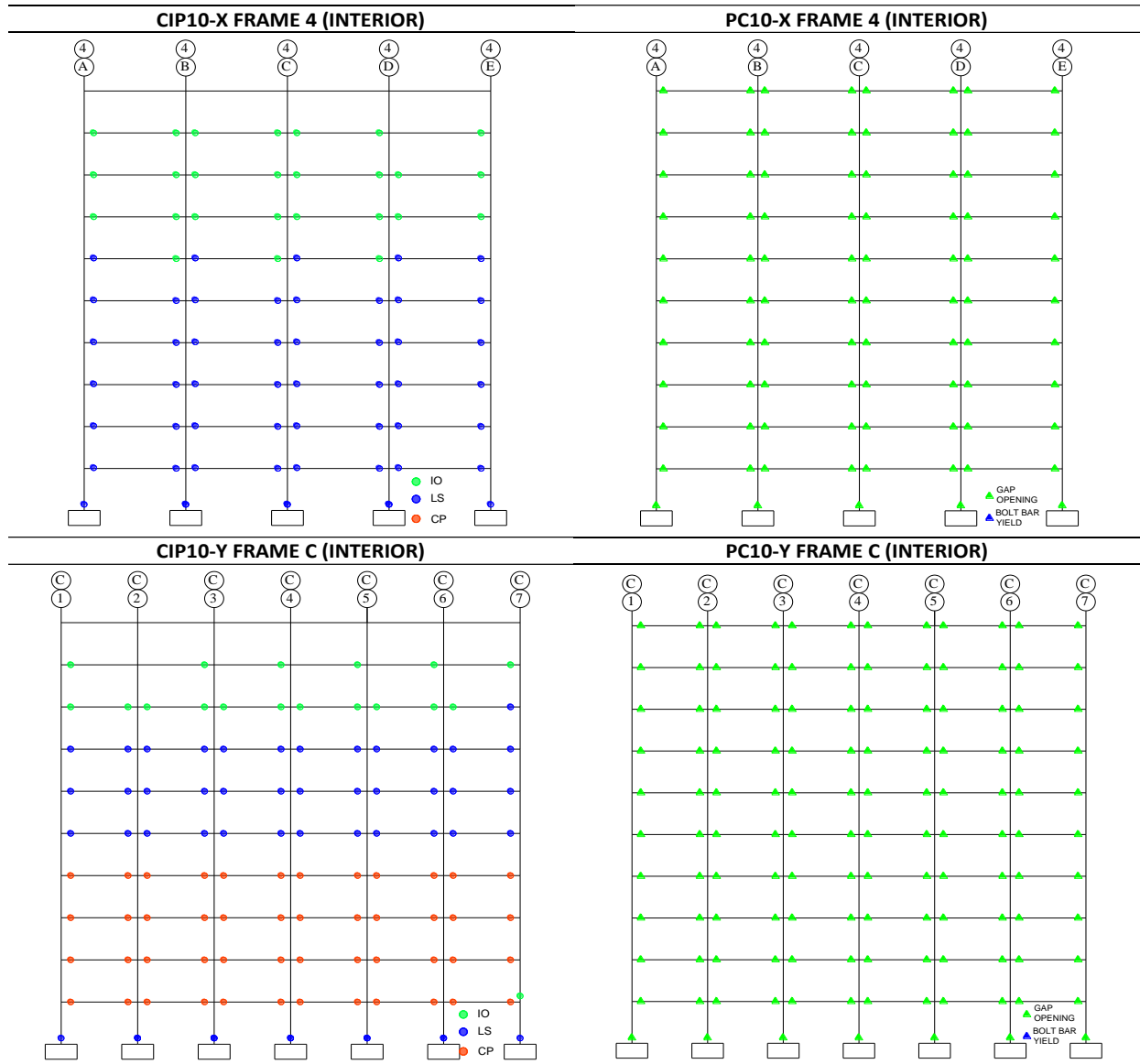


**Figure 8.** Hysteresis Curves of CIP10 (left) and PC10 (right) X Direction Beams

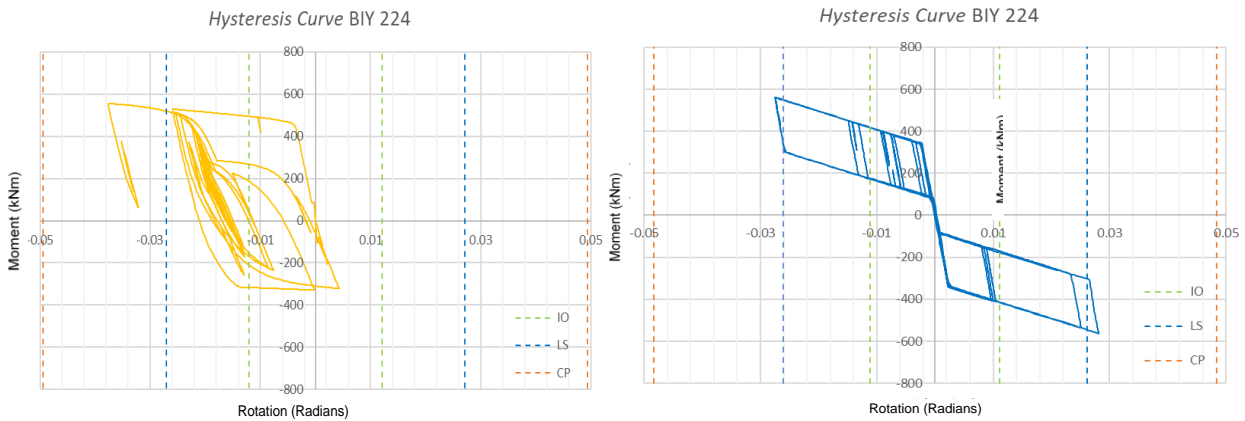


**Figure 9.** Hysteresis Curves CIP10 (left) and PC10 (right) Y Direction Beams

In order to evaluate the performance of the hybrid beam-column connections against conventional monolithic beam-column connections, element hysteresis curves of each building were also examined. Based on the results, a few samples of hysteresis curves of 10 story buildings' elements from the second scheme were chosen to be displayed in this paper. As depicted in Figures 8 and 9, although the beam hysteresis curves of CIP10 building display high energy dissipation capabilities, severe permanent deformation can be observed. This is caused by longitudinal rebar yielding which contributes to energy dissipation capabilities. On the other hand, hybrid beam-column connections exhibit flag-shaped hysteresis curves, which display considerable energy dissipation capabilities with self-centering traits. This is due to the presence of sacrificial external steel dissipation devices and unbonded post-tensioning tendons. The external mild steel bars were designed with lower capacities compared to the main precast concrete elements, and thus damages can be avoided on the precast concrete elements. During earthquake, mild steel bars would reach their yielding points and dissipated energy. Therefore, despite reaching higher rotation values, the connections were recorded to return to their initial position with negligible residual deformations. After earthquake, mild steel bars can be easily replaced to restore the structural performance of PC buildings. This is clearly a major advantage of PC buildings since CIP buildings can hardly be repaired after a strong earthquake event.

From the analysis results, it can be concluded that precast concrete structures experience lower degree of structural damages as compared to cast in place concrete structures. After severe earthquakes, replacement of energy dissipation devices and re-tensioning of unbonded post-tensioning tendons can be done to restore the structural performance of precast concrete structures. On the other hand, cast in place concrete structures can hardly be repaired and they may need to be demolished and re-built.

Thus, cost and duration of required repair or re-built can be significantly lower for precast concrete structures. Therefore, with lower building downtime, precast concrete structures could act as a more economical alternative in the long run.

## Conclusions

The seismic performance evaluation results of precast concrete buildings with hybrid *Damage Avoidance Design* connections have been presented. Comparisons have also been made with conventional cast in place concrete buildings. From these results, several concluding remarks can be listed as follows:

1. The designed precast concrete structures with hybrid *Damage Avoidance Design* connections proposed by Solberg et al. [4] require higher quantities of reinforcement compared to conventional cast in place concrete buildings. This is crucial to ensure that precast concrete elements are capable to withstand full connection capabilities, as stated in the strong column-strong beam-weak connection design philosophy.
2. The evaluated precast concrete structures tend to be more flexible compared to their monolithic cast in place counterparts, as indicated by the higher maximum roof displacements in most of the cases, except in the X-direction of the five story buildings.
3. There is no significant difference in terms of maximum interstory drift ratios between cast in place and precast concrete buildings. Moreover, all buildings satisfy the maximum interstory drift ratio limit of 4% as stated by ASCE 7-16 [13] under  $MCE_R$  level earthquakes.
4. Precast concrete buildings show their superiority by having significantly lower residual displacements, which on average are 97.4% lower than cast in place concrete buildings, indicating significantly lower degree of structural damages.
5. The hysteresis curves of precast concrete elements display the capability of the hybrid connections to maintain their flag-shaped hysteresis during

earthquakes, which allows considerable energy dissipation with ensured self-centering properties. Therefore, precast beam-column connections have significantly lower residual deformations as compared to conventional cast in place beam-column connections.

## References

1. Li, L., *Further Experiments on the Seismic Performance of Structural Concrete Beam-column Joints Designed in Accordance with the Principles of Damage Avoidance*, (Master's Thesis), University of Canterbury, 2006.
2. Priestley, M.J.N., Sritharan, S., Conley, J.R., and Pampanin, S., Preliminary Results and Conclusions from the PRESSS Five-storey Precast Concrete Test Building, *PCI Journal*, 44(6), 1999, pp. 43-67.
3. Mander, J.B. and Cheng, C.T., *Seismic Resistance of Bridge Piers based on Damage Avoidance Design*, Technical Report NCEER-97-0014, National Center for Earthquake Engineering Research, 1997.
4. Solberg, K., Dhakal, R., Mander, J., Li, L., and Bradley, B., Seismic Performance of Damage-protected Beam-column Joints, *ACI Structural Journal*, 105(2), 2008, pp. 205-214.
5. Solberg, K.M., *Experimental and Financial Investigations into the Further Development of Damage Avoidance Design*, (Master's Thesis). University of Canterbury, 2007.
6. SNI-03-1727-2020, *Beban Minimum untuk Perencanaan Bangunan Gedung dan Struktur Lain*, Badan Standarisasi Nasional, 2020.
7. ACI 318-14, *Building Code Requirements for Structural Concrete and Commentary*, American Concrete Institute, 2014.
8. SNI-03-2847-2019, *Persyaratan Beton Struktural untuk Bangunan Gedung*, Badan Standarisasi Nasional, 2019.
9. Christopoulos, C., Tremblay, R., Kim, H.-J., and Lacerte, M., Self-Centering Energy Dissipative Bracing System for the Seismic Resistance of Structures: Development and Validation, *Journal of Structural Engineering*, ASCE, 134(1), 2008, pp. 96-107.
10. Margono, I.K. and Atmajaya, P.K., *Perkuatan Terhadap Gempa Menggunakan Self-centering Energy Dissipation Braces pada Bangunan Ruko Empat Lantai Tidak Beraturan yang Direncanakan Terhadap Beban Gravitasi*, Bachelor's Thesis, Universitas Kristen Petra, 2011.
11. Scott, M. H., *Beam with Hinges Element*, [https://oensees.berkeley.edu/wiki/index.php/Beam\\_With\\_Hinges\\_Element](https://oensees.berkeley.edu/wiki/index.php/Beam_With_Hinges_Element), 2014.
12. ASCE 41-17, *Seismic Evaluation and Upgrade of Existing Buildings*, American Society of Civil Engineers, Reston, Virginia, 2017.
13. ASCE 7-16, *Minimum Design Loads and Associated Criteria for Buildings and Other Structures*, American Society of Civil Engineers, Reston, Virginia, 2017.